

I-SEEC2011

## Structure and Surface Morphology of Cr-Zr-N Thin Films Deposited by Reactive DC Magnetron Sputtering

C. Chantharangsi<sup>a\*</sup>, S. Denchitcharoen<sup>a</sup>, S. Chaiyakun<sup>b,c</sup>, P. Limsuwan<sup>a,c</sup>

<sup>a</sup>Department of Physics, Faculty of Science, King Mongkut's University of Technology Thonburi, Bangkok, 10140, Thailand

<sup>b</sup>Vacuum Technology and Thin Film Research Laboratory, Department of Physics, Faculty of Science, Burapha University, Chonburi, 20131, Thailand

<sup>c</sup>Thailand Center of Excellence in Physics, CHE, Ministry of Education, Bangkok 10400, Thailand

**Elsevier use only:** Received 30 September 2011; Revised 10 November 2011; Accepted 25 November 2011.

### Abstract

In this study, chromium zirconium nitride (Cr-Zr-N) thin films have been prepared by reactive dc closed field unbalanced magnetron co-sputtering on Si (100) wafers and glass slides for 60 min without substrate heating and biasing voltage in gas mixture of Ar and N<sub>2</sub> with flow rates kept constant at 3.0 sccm and 6.0 sccm, respectively. The sputtering currents applied to Zr target were varied from 0.2 A to 0.8 A, whereas the current of Cr target was kept at 0.8 A. To investigate films structure and surface morphology as a function of Zr content, the as-deposited films were characterized by X-ray diffraction (XRD), atomic force microscopy (AFM), field emission scanning electron microscopy (FE-SEM), and energy-dispersive X-ray spectroscopy (EDX). The results suggested that increasing in current applied to Zr target enhanced the deposition rate and also increased Zr content in the films ranging from 6.0 to 31.2 at %. The films formed a solid solution (Cr, Zr)N where Zr atoms substitute Cr atoms in the CrN lattice. The lattice parameters increased from 0.4207 nm to 0.4357 nm, whereas the grain sizes decreased from 11.27 nm to 7.412 nm. The film structure developed with the coexistence of (111) and (200) crystallographic orientation into a mixture of nanocrystalline grains as the sputtering currents of Zr target exceeded 0.2 A. The AFM images showed smoothing surface morphology with the roughness decreased from 9.471 nm to 2.437 nm. Cross-sectional micrographs exhibited the microstructure evolution corresponding to the grain refinement as a result of increasing Zr discharge current.

© 2010 Published by Elsevier Ltd. Selection and/or peer-review under responsibility of I-SEEC2011  
Open access under [CC BY-NC-ND license](https://creativecommons.org/licenses/by-nc-nd/4.0/).

**Keywords:** Cr-Zr-N; Solid Solution; Magnetron Sputtering

\* Corresponding author. Tel.: +6-689-058-5527; fax: +662-872-5254.  
E-mail address: [jiphysics@gmail.com](mailto:jiphysics@gmail.com).

## 1. Introduction

Nowadays, the surface coating with hard material is the commercial interest because it can be used to extend the lifetime of machine components and tools and to make engines and devices more efficient. The binary nitride thin films such as TiN, CrN, and ZrN have been most extensively studied and frequently used in various industries because of their high hardness, good wear resistance, low friction coefficient, and excellent corrosion resistance. However, the binary nitride is still not good enough for some specific applications. For example, in the case of high speed machining, the mechanical properties of CrN film are degraded rapidly by the formation of porous oxides at the film surface during service at high temperature above 700°C [1]. Moreover, the coarse columnar grain structure of CrN and TiN films could have many voids and other structural defects, which could be an oxygen diffusion path [2]. In order to overcome these problems, ternary nitride thin films with the addition of other elements into binary system have been developed, and their superior properties to the binary nitride system have been reported in many papers. Among these films, Cr-based ternary nitride coatings such as Cr-Ti-N [3], Cr-Al-N [4], Cr-W-N [5], Cr-Si-N [6], and Cr-Zr-N [7-9] have been extensively studied due to high temperature oxidation resistance of CrN films, especially Cr-Zr-N films. Many research groups reported that the films have been much improved not only the mechanical properties, but also the very low surface roughness with increasing Zr content [7]. However, most of previous studies have necessarily used the substrate heating and/or substrate biasing to improve the film structure. These techniques can give rise to the heating effects of substrate which lead to higher production cost for industry. Therefore, it is important and commercially useful to study the sputter deposition of these films without heating and biasing the substrates.

In this paper, Cr-Zr-N thin films were prepared by using reactive dc unbalanced magnetron sputtering without substrate heating and voltage biasing at a long distance from the targets. Their structure and surface morphology were investigated as a function of Zr contents.

## 2. Experiment

The Cr-Zr-N films were prepared by closed field unbalanced magnetron sputtering system. These films were deposited on silicon (100) wafers and glass slides without external heating and voltage biasing. In this system, the 99.99% metallic Cr and Zr targets with diameter of 3 inches were used as the magnetron sources. The targets were installed on the wall of cylindrical chamber. The substrate holder was placed vertically at the center of the chamber and separated from each target as a distance of 13 cm. Prior to films deposition, the sputtering chamber was evacuated to the base pressure of  $5.0 \times 10^{-5}$  mbar by a diffusion pump accompanied with a rotary pump. The targets were pre-sputtered in Ar atmosphere for 10 min to remove contaminants from the surface. After target cleaning, the deposition of films was performed in a mixture of Ar-N<sub>2</sub> atmosphere at the constant working pressure of  $4.0 \times 10^{-3}$  mbar by keeping the flow rate of Ar (99.999%) and N<sub>2</sub> (99.999%) gas at 3.0 and 6.0 sccm, respectively. To produce the films with various Zr contents, the sputtering current of the Zr target was varied from DC 0.2 and 0.8 A while that of the Cr target was maintained at DC 0.8 A. Deposition time was fixed at 60 min for each.

The chemical composition of films was determined from energy-dispersive X-ray spectroscopy (EDS2006 550i Analyzer). The crystal phase and texture of films were characterized by X-ray diffraction (Rigaku, Rint 2000) using CuK $\alpha$  radiation ( $\lambda=1.542$  nm) operated at 40 kV and 40 mA with a glancing angle of incidence (3°). The XRD pattern was recorded from 20° to 80° with  $2\theta$  scanning rate of 2° min<sup>-1</sup>. The surface morphology, roughness, and film thickness were observed by an atomic force microscope (Nanoscope IV, Veeco Instrument Inc) on a scanning area of  $1 \times 1 \mu\text{m}^2$ . The cross-sectional morphology was investigated by field emission scanning electron microscopy (FE-SEM, HITACHI S-4700).

### 3. Results and discussion

#### 3.1. Chemical composition

The atomic concentrations of Cr, Zr and N on the films deposited with various discharge current of Zr target were determined from EDX analysis and listed in Table 1. The Zr content increased from 6.01 to 31.15 at % with increasing Zr target current, whereas the nitrogen content decreased from 43.72 to 27.65 at %. This is a result of keeping the nitrogen at a fixed flow rate despite the increase in the Zr discharge current. Moreover, increasing of energetic particles bombarding onto the surface of growing film could result in desorption of the nitrogen and thus in the decrease of its content [10].

Table 1. Chemical composition of the Cr-Zr-N films as a function of the discharge current of Zr target

| Discharge current of Zr target (A) | Chemical composition (at.%) |       |       |
|------------------------------------|-----------------------------|-------|-------|
|                                    | Cr                          | Zr    | N     |
| 0.2                                | 50.27                       | 6.01  | 43.72 |
| 0.4                                | 47.83                       | 16.20 | 35.97 |
| 0.6                                | 44.37                       | 21.78 | 33.85 |
| 0.8                                | 41.20                       | 31.15 | 27.65 |

#### 3.2. Crystalline structure

Figure 1 shows X-ray diffraction pattern of Cr-Zr-N coatings on Si (100) with different Zr target currents. The absence of separate sets of diffraction peaks for CrN and ZrN from the XRD pattern suggested that these films exhibited the single-phase crystalline structure of fcc NaCl-type. This could be attributed to the similarities between CrN and ZrN crystalline structures and fairly good mutual solubility of zirconium in the chromium metal [11]. As the Zr target current increases, these peaks gradually shifted toward the lower  $2\theta$ -position. This result suggested that the films formed a solid solution (Cr, Zr)N whereby Cr atoms are substituted by Zr atoms. The lattice parameters of these films, which were deduced from the (111) peaks, increase from 0.4207 nm to 0.4357 nm with increasing Zr target current, as shown in Fig. 2. The increase in the lattice parameters could be the results of the substitution of Cr with Zr in the CrN lattice since the radius of Zr atom (0.161 nm) is larger than the radius of Cr atom (0.136 nm) [7]. These results are consistent with those reported by other researchers [7-9]. Furthermore, the increase in Zr target current could result in the development of crystallographic orientation in the films. The films exhibited strong (111) preferred orientation at the Zr discharge current of 0.2 A and became a mix-phase of (111) and (200) crystallographic orientation at the higher currents (0.4 – 0.8 A). This result suggested that increasing Zr target current lead to the increase in flux of energetic particles impinging on the film surface. With the energetic bombarding, higher adatom mobility and resputtering can cause surface rearrangement. For NaCl structure, grains with  $\langle 100 \rangle$  direction are the most open channeling. Along this direction the energy of impinging particles is distributed over larger volumes leading to lower sputtering yields and less lattice distortion. Therefore, The grains with (200) plane have more probabilities for survival and (200) texture can be developed [12-13].

The grain sizes were calculated from the full width at half maximum of the XRD peaks by using the Scherrer formula and plotted against the Zr target current as shown in Fig. 3. This figure indicated that grain refinement occurred as a result of the increasing Zr target current.

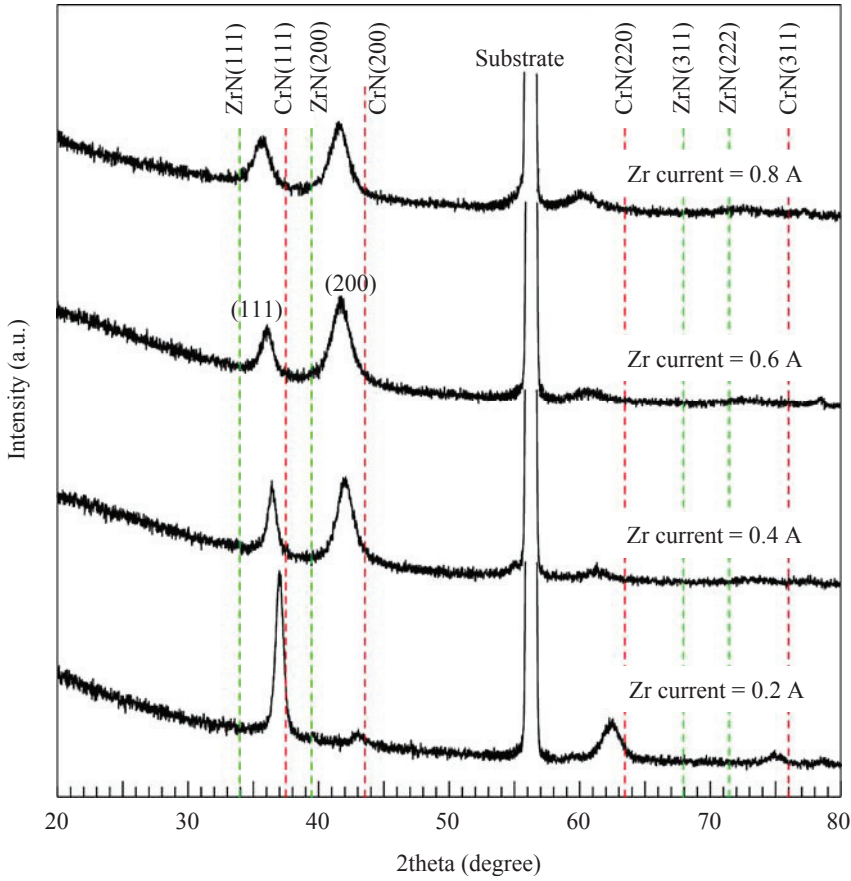


Fig. 1. X-ray diffraction patterns of Cr-Zr-N films with various Zr discharge currents

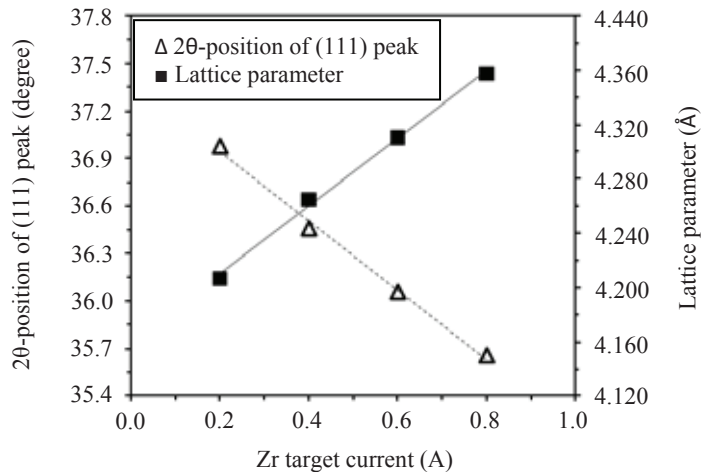


Fig. 2. Lattice parameter and 2θ-position of (111) peak of the Cr-Zr-N films as a function of the Zr target current

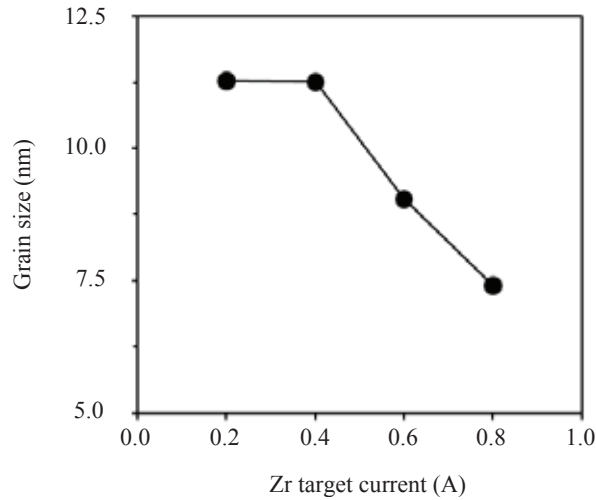


Fig. 3. Grain sizes determined from the FWHM of (111) peaks by using the Scherrer formulas as a function of Zr target current

### 3.3. Surface morphology

Figure 4 shows AFM surface images of the films with different Zr target currents. As shown in Fig. 4, the films exhibited smoothing surface with increasing Zr discharge current. The root-mean-square (RMS) roughness from AFM analysis was decreased from 9.471 nm to 2.437 nm and corresponded to decreased grain sizes determined from XRD pattern.

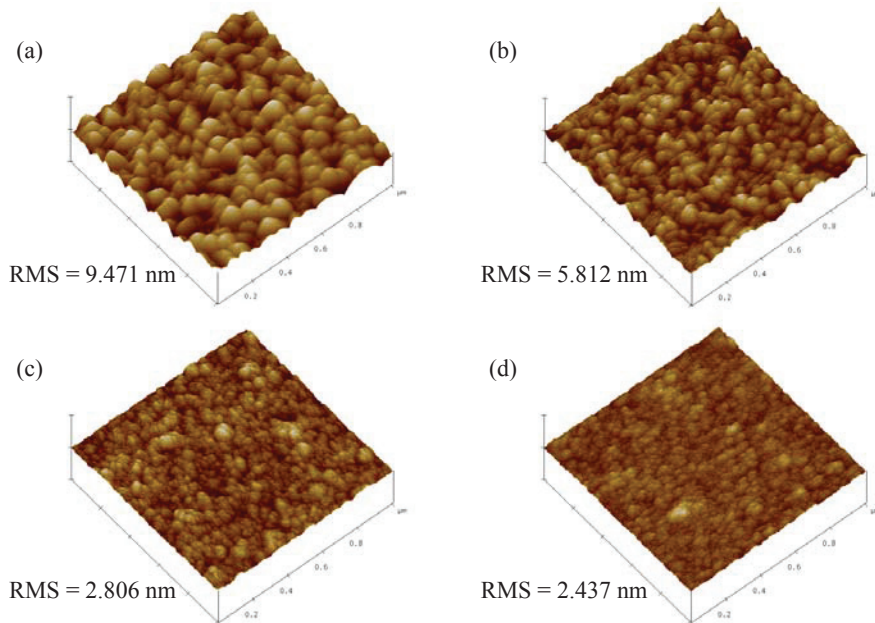


Fig. 4. AFM surface morphologies and RMS roughness of the Cr-Zr-N films: (a) 0.2 A; (b) 0.4 A; (c) 0.6 A; (d) 0.8 A

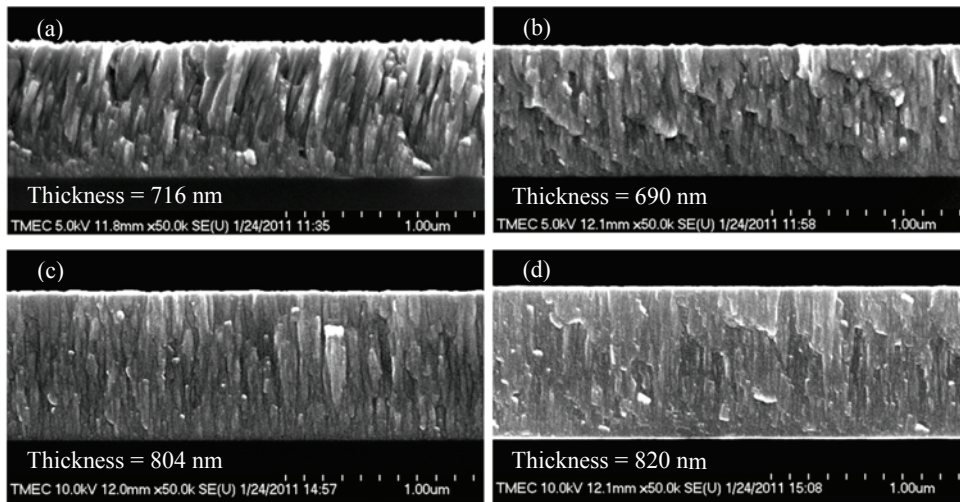


Fig. 5. Cross-sectional SEM morphologies of the Cr-Zr-N films: (a) 0.2 A; (b) 0.4 A; (c) 0.6 A; (d) 0.8 A

Figure 5 represents the fracture cross-section of these films. These photographs showed the development of film microstructure with the increase in Zr target current. The low adatom mobility caused by the low energy flux on the film with Zr current of 0.2 A results in competitive growth of grains and open grain boundaries. This process can result in a thicker film with porous microstructure corresponding to Zone 1 in Thornton's structure zone model. As the Zr target current increased, bombarding with higher energetic particles lead to the microstructure with densely packed fibrous grains which correspond to Zone T in the zone model. In addition, the Zr atoms added to the films can result in the dense microstructure through the grain refinement. Refining grains are the effects of impurities or additives in the film that predicted by the Barna and Adamik's structure zone model [14]. According to this model, Zr atoms added to the films stop the grain growth and stimulate the renucleation of grains. These results are in agreement with the smoothing surface morphology and the grain size decreasing of the films.

#### 4. Conclusions

CrZrN films were prepared by using reactive dc unbalanced magnetron sputtering without substrate heating and bias. The structure and surface morphology of these films were evaluated as a function of Zr target current. XRD analysis revealed that the films formed nanocrystalline solid solution (Cr, Zr)N where Zr atoms substituted Cr atoms in CrN lattice. Their lattice parameters increase from 0.4207 nm to 0.4357 nm with increasing Zr content, whereas the grain sizes decrease from 11.27 nm to 7.412 nm. The increase in energy flux with increasing Zr discharge current could result in crystallographic orientation development. The films exhibited a mixture of nanocrystalline grains of the coexistence of (111) and (200) crystallographic orientation as the Zr target current exceeded 0.2 A. AFM analysis shows smoothing surface morphology with roughness decreased from 9.471 nm to 2.437 nm. Cross-sectional micrographs from FE-SEM exhibited the microstructure evolution corresponding to smoothing surface morphology. The increase in Zr discharge current leads to the increase in energy flux and Zr content and results in the formation of a nanocomposite structure which favors grain refinement during the growth process.

## Acknowledgement

The author would like to thank Vacuum Technology and Thin Films Research Laboratory, Burapha University for providing the sputtering instruments and Dr. A. Buranawong for XRD measurement. This research was supported by KMUTT under the National Research University project.

## References

- [1] Zeng XT, Zhang S, Sun CQ, Liu YC. Nanometric-layered CrN/TiN thin films: mechanical strength and thermal stability. *Thin Solid Films* 2003;**424**:99-102.
- [2] Arias DF, Marulanda DM, Baena AM, Devia A. Determination of friction coefficient on ZrN and TiN using lateral force microscopy (LFM). *Wear* 2006;**261**:1232-1236.
- [3] Hones P, Sanjinés R, Lévy F. Sputter deposited chromium nitride based ternary compounds for hard coatings. *Thin Solid Films* 1998;**332**:240-246.
- [4] Uchida M, Nihira N, Mitsuo A, Toyoda k, Kubota k, Aizawa T. Friction and wear properties of CrAlN and CrVN films deposited by cathodic arc ion plating method. *Surf Coat Technol* 2004;**177-178**:627-630.
- [5] Hones P, Diserens M, Sanjinés R, Lévy F. Electronic structure and mechanical properties of hard coatings from the chromium–tungsten nitride system. *J Vac Sci Technol B* 2000;**18**:2851-2856.
- [6] Martinez E, Sanjinés R, Karimi A, Esteve J, Lévy F. Mechanical properties of nanocomposite and multilayered Cr–Si–N sputtered thin films. *Surf Coat Technol* 2004;**180-181**:570-574.
- [7] Kim GS, Kim BS, Lee SY, Hahn JH. Structure and mechanical properties of Cr-Zr-N films synthesized by closed field unbalanced magnetron sputtering with vertical magnetron sources. *Surf Coat Technol* 2005;**200**:1669-1675.
- [8] Aouadi SM, Maeruf T, Twesten RD, Mihut DM, Rohde SL. Physical and mechanical properties of chromium zirconium nitride thin films. *Surf Coat Technol* 2006;**200**:3411-3417.
- [9] Zhang ZG, Rapaud O, Bonasso N, Mercs D, Dong C, Coddet C. Microstructures and corrosion behaviors of Zr modified CrN coatings deposited by DC magnetron sputtering. *Vacuum* 2008;**82**:1332-1336.
- [10] Cavaleiro A, Hosson JTMD. *Nanostructured coatings*. New York: Springer; 2006.
- [11] Fox-Rabinovich GS, Bushe NA, Kovalev AI, Korshunov SN, Shuster LS, Dosbaeva GK. Impact of ion modification of HSS surfaces on the wear resistance of cutting tools with surface engineered coatings. *Wear* 2001;**249**:1051-1058.
- [12] Abadias G. Stress and preferred orientation in nitride-based PVD coatings. *Surf Coat Technol* 2008;**202**:2223-2235.
- [13] Martin PM. *Handbook of Deposition Technologies for Films and Coatings*. 3rd ed. New York: William Andrew; 2009.
- [14] Petrov I, Barna PB, Hultman L, Greene JE. Microstructural evolution during film growth. *J Vac Sci Technol* 2003;**21**:S117-S128.